Characterization of 1 cm^2 Low Gain Avalanche Diodes for Space Applications

Cavazzini Leo, Abstract ID: 230

Department of Physics, University of Trento, via Sommarive 14, I-38123 Trento, Italy
Fondazione Bruno Kessler

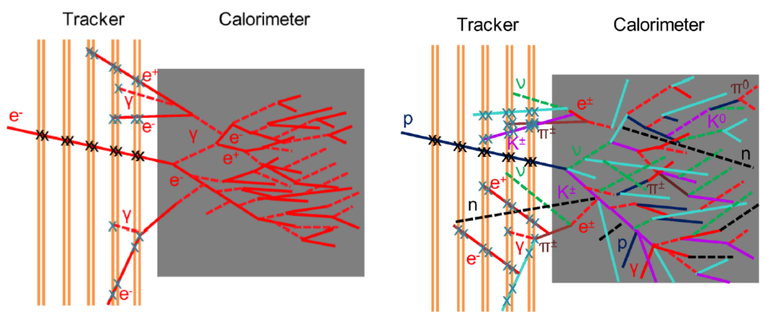

Figure 1. *Schematic representation of the back-scattered secondary particles from the calorimeter into a tracking detector system. (Left) An electromagnetic shower generated by primary electrons in the calorimeter may feature only ultra-relativistic γ and $e^{\pm}$ in the upstream detectors. (Right) Heavier particles like protons generate a hadronic shower in the calorimeter, which features slow secondary particles. For a sufficient high energy, the signal from the primaries can be overwhelmed by the background of secondaries*

Introduction

To measure the energy and the momentum of Charged Cosmic Rays (CCRs) in space is often used a solid-state tracker coupled with a calorimeter, like in **Figure 1**. For these, the energy deposited by the primary particles cannot be separated from the energy deposited by the back-scattered secondaries, but it has been shown that measuring the timing of charged particles crossing the tracker layers with a precision of less than 100 ps can help separate the primary from the secondary particles. The Low Gain Avalanche Diodes (LGADs) are silicon detectors used in High Energy Physics (HEP) with an internal gain of $\mathcal{O}(10)$ capable of achieving a timing resolution of $\sigma \sim 30$ *ps*. A schematic sketch of an LGAD is shown in **Figure 2**. The typical active area of these sensors is of the order of $\mathcal{O}(1\ \text{mm}^2)$ with a thickness of 50 µm whereas space experiments use micro-strip sensors having a channel size of about 1 cm^2. This work aims to prove that it is possible to produce LGADs with areas in the order of 100 mm^2, with timing resolution below 100 ps.

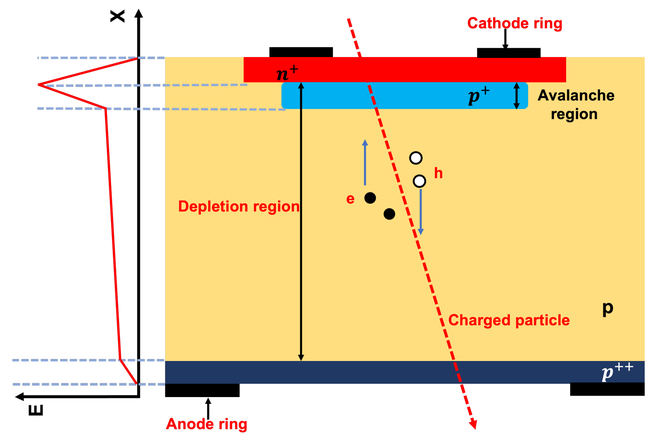

Figure 2. *Cross section of a Low Gain Avalanche Diode. The peak in the electric field corresponds to the gain region where the mobile charges drift with sufficient energy to trigger a multiplication. Signal is induced in the electrodes by the charge movement.*

Simulations

An LTspice simulation was performed to estimate the jitter for different combinations of gain and thickness when the channel size is increased from 1 mm^2 to 1 cm^2. One of the most important limitations to the performance of timing detectors is their jitter. **Figure 3** gives a visual representation of the jitter as calculated using the equation:

$$\sigma_{Jitter} = \frac{\sigma_{Noise}}{Slew\ Rate\ (dV/dt)} \quad , \tag{1}$$

where the slew rate was calculated by determining the ratio between the amplitude and the signal peaking time, while the noise contribution of the sensor is restricted to the shot noise and a constant contribution due to the electronics. According to **Figure 3**, jitter values below 50 ps can be achieved for a channel size of 1 cm^2 having a sensor thickness above 100 µm and a gain around 100. Based on these results, a batch of LGADs was produced, with an active thickness of 100 µm and 150 µm, named in the paper wafers 8, 9 and wafers 12, 14 respectively.

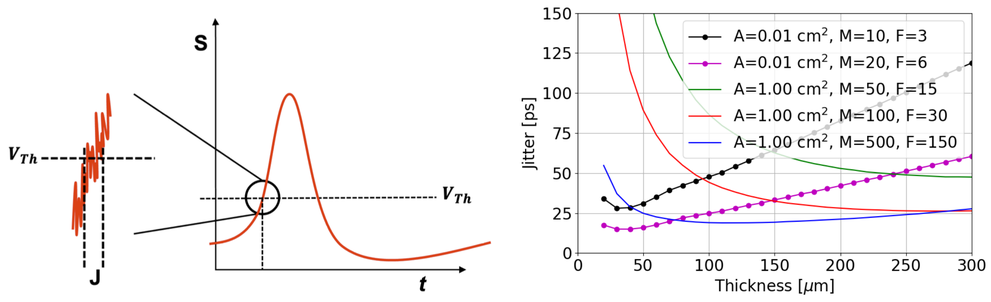

Figure 3. *(Left) The uncertainty in time for a signal to cross a threshold due to noise is called jitter (J). (Right) LTspice simulation of jitter as a function of the thickness, for different areas (A), gain (M) and the excess noise factor (F). The black and purple markers represent the standard LGADs used in HEP.*

Experimental method: Transient Current Technique

In TCT, an IR pulsed laser can simulate the passage of CCRs through the sensor with tunable energy. For this study, the IR laser was calibrated to 1 MIP. The setup includes a beam monitor that continuously measures the laser intensity. The data from the beam monitor were used to normalize the sensors' charge to reduce the effect of laser fluctuations as much as possible. Look at **Figure 4** for a sketch of the main instruments.

The collected charge from sensors is measured by illuminating them with the IR laser and integrating the signal over time, which is then divided by the output impedance. To estimate the gain, the charge for both an LGAD and an equivalent PIN diode (i.e. with the same geometry and layout) is estimated as a function of bias voltage. The gain is defined as:

$$Gain|_{V_{bias}} = \left.\frac{Q_{LGAD}}{Q_{PIN}}\right|_{V_{bias}} \tag{2}$$

where Q_{LGAD} and Q_{PIN} are the collected charge by the LGAD and PIN sensors respectively. The gain measurements for 100 mm^2 LGADs are shown on the left panel of **Figure 5** as a function of the bias voltage at room temperature.

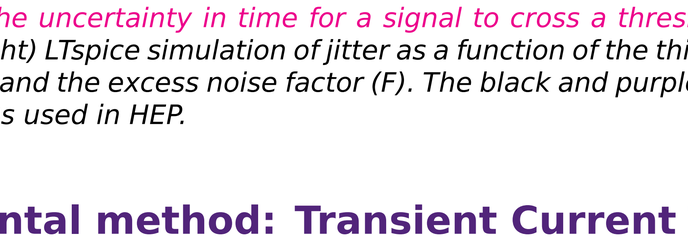

Figure 4. *Schematic view of the Transient Current Technique setup.*

To quantify the jitter, two measurements were conducted for each sensor: the first aimed to quantify the slew rate by averaging 256 waveforms in the oscilloscope, while the second was dedicated to estimating the noise, involving no averaging. The noise is defined as the standard deviation of fluctuations of the waveform around the baseline preceding the signal from the IR laser pulse. The jitter is calculated using **Equation 1**.

Another issue to address with the large area sensors is the uniformity of signal shape across the active area. For that, the laser is used to create charge carriers at different distances from the position of the wire bond connecting the sensor to the readout electronics, using the different metal openings. Any variation in the arrival time of the signal at the oscilloscope is measured by a Constant Fraction Discrimination algorithm with a threshold set at 50% of the amplitude. This measurement comprises both the contribution of variation in the signal shape (different rise-time) and in the signal propagation within the sensor. To remove the first contribution, the difference between the maximum and minimum arrival time is computed, and plotted in **Figure 6** as a function of the bias voltage.

Results and Prospects

By measuring a set of 1 cm^2 LGADs it was observed that: **Wafer 9** and **Wafer 14** are the only ones reaching lower values than the two threshold lines marking 100 ps (solid) and 50 ps (dashed), while wafer 12 goes below the first, making those the most promising designs. Wafer 14 achieves the best jitter value of about 34 ps at 400 V when the gain is close to 40. However, Wafer 9 archives an equivalent value of jitter i.e., 36 ps at 300 V and gain 32. These values show that a difference of 100 V is required to achieve similar performance in the thicker sensor.

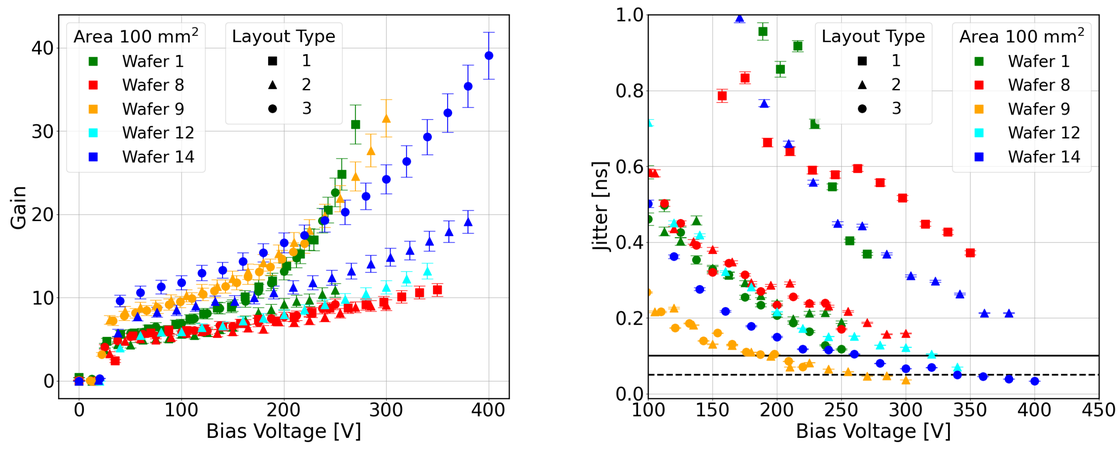

Figure 5. *Measurements using a pulsed IR laser impinging on 1 cm^2 pad sensors of different thicknesses, as a function of the bias voltage: gain, calculated with Equation 2 (left), jitter calculated with Equation 1 (right). Samples marked as Wafer 1 are 50 µm thick.*

The uniformity of the signals was probed for the most promising sensors. **Figure 6** illustrates the difference between the maximum and minimum arrival times measured for two types of 100 µm LGADs. In the operating voltage region of the sensor, the spread remains constant while varying the bias voltage. For the Type-2 sensor the contribution of the arrival time to the timing resolution is estimated as

$$\sigma_{uni} = \frac{153}{\sqrt{12}}\ ps \approx 44\ ps \tag{3}$$

where the numerator represents the mean value of arrival time spread and the denominator accounts for the assumption of a uniform distribution of particles on the detector. The spread obtained needs to be added to the jitter exhibited by the sensors when calculating the timing performances. The time resolution due to jitter and non-uniformity of the signal shape for the LGAD with an active area of 1 cm^2, 100 µm thick, at 300 V is estimated as

$$\sigma_t = \sqrt{\sigma^2_{Jitter} + \sigma^2_{uni}} = \sqrt{36^2 + 44^2}\ ps \approx 57\ ps \tag{4}$$

This shows that the effect of non-uniformity plays a significant role in the timing performance of the larger sensors. Although, the different values of Type-2 and Type-3 do not follow the expected trend from the layout design. In fact, Type-2 sensors present contacts only around their perimeter, while Type-3 present contact holes spread across the active area (see **Figure 6**). As a result, it was anticipated an improvement due to the reduced resistance from spread contacts.

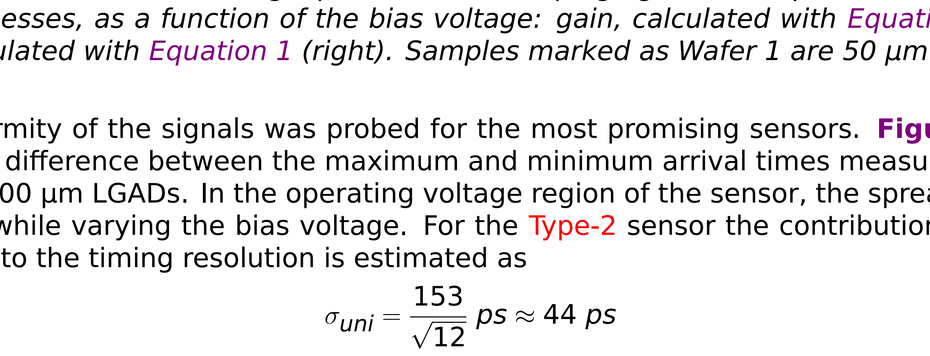

Figure 6. *(Left) Layout of a Type-3 Sensor: blue layers represent the metallization, black are contact holes and white squares are injection openings. (Right) Arrival time spread generated in different positions across the sensor as a function of bias voltage for two sensors of 1 cm^2 area and thickness 100 µm.*

The outcomes are encouraging on the one side but still challenging on the other. To further investigate the signal propagation properties and to break the 100 gain "barrier", a new batch of Space LGADs is under production and will be tested in the next year in FBK. In the meantime, the facilities of the SSD group at CERN are used to dig deeper into the results.

Many greetings: to all the people from the Custom Radiation Sensors group from FBK for their support and enthusiasm in sharing their knowledge; to the organizers of this event; and to the CERN-SSD group.